Journal of Advanced Engineering Trends
ISSN : 2682 - 2091

Vol.42, No.2. July2023

http://jaet.journals.ekb.eg

SHEAR STRENGTH OF LOW VOLUME STEEL FIBER CONCRETE UNDER STATIC OR REPEATED LOADS

Yasser R. Tawfic[1], Mohamed Y. Farid[1], Kamal A. Assaf[2], L. M. Abd-elhafez[1]

[1]Civil Engineering Department, Minia University, Egypt
[2]Civil Engineering Department, Assuit University, Egypt

Abstract

Studies have shown that steel fibers improve concrete performance specially shear and tensile strength. The degree of improvement gained depends mainly on the type, shape and volume of the steel fibers. The main objective of this study is to investigate the shear behavior of low volume content steel fiber concrete under static or repeated loading. Low volume steel fibers ($V_f < 1$ %) presents an economic solution that guaranties suitable workability for concrete. Three groups with a total number of one hundred twenty-six push-off concrete specimens were casted and tested. The experimental variables were the concrete compressive strength, the shape of the steel fibers (corrugated or hooked end steel fiber), the volume content of the steel fiber (0.15, 0.30 and 0. 45%) and the type of loading (static or repeated). The experimental test results showed up to 30% increase for the shear capacity of the concrete as well as an increase for the fatigue life due to the presence of low volume content of steel fibers. An equation is proposed to predict the fatigue life of the steel fiber concrete.

Keywords: Steel fibers, concrete, shear strength, repeated loading, fatigue life.

1. Introduction

Shear failure of concrete structures is brittle and sometimes catastrophic so that the presence of steel fibers as shear reinforcement is recommended to improve the overall behavior of concrete. Previous researches, Higashiyama and Banthia (1); Majdzadeh et al. (2); Mirsayah and Banthia (3); Valle and Buyukozturk 1993(4); Narayanan and Darwish 1987 (5) have shown that the presence of steel fibers contribute to the shear performance of plan concrete by increasing its tensile strength and ductility as well as controlling the cracks initiation and propagation.

Fatigue is a parameter that represents the number of cycles the material can withstand under a given pattern of repetitive loading up to failure. High cyclic loading is characterized by a large number of cycles at low stress levels (from 10^3 to 10^7 cycles). On the other hand, low-cyclic loading involves the application of less than one thousand number of load cycles at high stress levels [RILEM Committee (6)]. Miguel Fernandez Ruiz et al. (7) studied the influence of fatigue loading on shear failure of reinforced concrete members (no transverse reinforcement) and they concluded that stress level below approximately 50 % of the static shear strength is not enough to cause the shear fatigue.
Investigating the shear fatigue response of cracked concrete interface, Esayas Gebreyouhannes et al. (8) reported that the degree of deterioration is found to be highly sensitive to the loading pattern and the loading amplitude level. Jun Wei Luo and Frank J. Vecchio (9) conducted experimental work to examine the behavior of steel fiber reinforced concrete under reversed cyclic shear. Test results showed that the fiber volume and the fiber aspect ratio significantly influence the shear performance of steel fiber reinforced concrete.

In order to investigate the shear strength, researches (3 and 10-14) utilized different types and shapes of push off test specimens that is capable of concentrating the shear stress along a narrow shear ligament producing pure shear on a defined and predetermined plan. This research study aims to characterize the shear behavior and fatigue life of the low volume steel fiber concrete by means of applying static or cyclic loads on Z-shape specimens.

2. Experimental Program

One hundred twenty-six push-off tests were carried out under static or repeated loads to investigate the shear strength properties of low volume content steel fiber concrete. The experimental variables were:

- Concrete compressive strength (250, 325 and 400 kg/cm^2).
- Steel fiber content (V_f %); three percentages of fiber volume contents (0.15%, 0.30% and 0.45%).
- Steel fiber shape; corrugated or hooked end shapes.
- Type of loading; static or repeated loads

2.1 Test Specimens

Revised:17 October, 2021, Accepted:14 December , 2021

Figure (1) shows a Z-shape push off test specimens with overall dimensions 25x15x15 cm. The area of the shear plane is 105 cm^2. The two main sides of the Z-shape specimens were reinforced using 6 mm diameter steel bars to ensure that failure happens through the shear plane. Tables (1) and (2) show the test program that consists of 42 test specimens divided into six categories. To ensure high accuracy, three elements were casted and tested for each specimen. Specimens in categories As, Bs and Cs were tested under direct static shear loading and specimens in categories Ar, Br and Cr were tested under repeated loading. Every category consists of seven specimens; one of them has zero fiber content to serve as a control specimen. The remaining six specimens have different shapes and volume of steel fibers. For every concrete patch, three cubes and three cylinders were casted, cured and tested to identify the concrete properties, see Table (3) and Table (4).

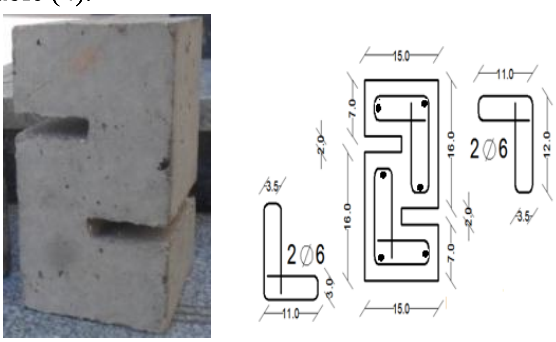

Figure (1): Geometry of the Z-Shape test specimens.

Table (1): Test specimens under static loading.

Category	Specimen	f_{cu} (kg/cm^2)	V_f (%)	Shape of Fiber	Load Type
As	As1	250	0.00	-	Static
	As2		0.15	Corrugated	
	As3		0.15	Hooked end	
	As4		0.30	Corrugated	
	As5		0.30	Hooked end	
	As6		0.45	Corrugated	
	As7		0.45	Hooked end	
Bs	Bs1	325	0.00	-	
	Bs2		0.15	Corrugated	
	Bs3		0.15	Hooked end	
	Bs4		0.30	Corrugated	
	Bs5		0.30	Hooked end	
	Bs6		0.45	Corrugated	
	Bs7		0.45	Hooked end	
Cs	Cs1	400	0.00	-	
	Cs2		0.15	Corrugated	
	Cs3		0.15	Hooked end	
	Cs4		0.30	Corrugated	
	Cs5		0.30	Hooked end	
	Cs6		0.45	Corrugated	
	Cs7		0.45	Hooked end	

Table (2): Test specimens under repeated loading.

Category	Speci-men	f_{cu} (kg/cm^2)	V_f (%)	Shape of Fiber	Load Type
Ar	Ar1	250	0.00	-	Repeated
	Ar 2		0.15	Corrugated	
	Ar 3		0.15	Hooked end	
	Ar 4		0.30	Corrugated	
	Ar 5		0.30	Hooked end	
	Ar 6		0.45	Corrugated	
	Ar 7		0.45	Hooked end	
Br	Br 1	325	0.00	-	
	Br 2		0.15	Corrugated	
	Br 3		0.15	Hooked end	
	Br 4		0.30	Corrugated	
	Br 5		0.30	Hooked end	
	Br 6		0.45	Corrugated	
	Br 7		0.45	Hooked end	
Cr	Cr1	400	0.00	-	
	Cr 2		0.15	Corrugated	
	Cr 3		0.15	Hooked end	
	Cr 4		0.30	Corrugated	
	Cr 5		0.30	Hooked end	
	Cr 6		0.45	Corrugated	
	Cr 7		0.45	Hooked end	

Table (3): Properties of the steel fibers.

Steel fibers	Width (mm)	Thickness (mm)	Φ equivle-nt (mm)	Length L_f (mm)	Aspect ratio (L_f/Φ)
Corrugat-ed	0.77	2.80	1.66	25.0	15
Hooked-end	0.53	1.92	1.14	24.3	21.3

Table (4): Mix details for all patches.

Concrete Mix. f_{cu} kg/cm^2	Cement kg/m^3	Sand kg/m^3	Gravel kg/m^3	W/C	Super-Plasticizer l/m^3
250	350	620	1240	45%	--
325	400	570	1140	40%	--
400	420	590	1180	40%	3.1

W/C :Water cement percentage

(a) Corrugated steel fiber. (b) Hocked end steel fiber.

Figure (2): Steel fibers.

2.2 Materials

Cement has 3.15 specific gravity was used for all concrete mixes. The cement 28 days compressive strength was 340 kg/cm^2. Nature fine and coarse aggregates from Minia western desert quarries were used. The maximum nominal size of the coarse aggregate was 20 mm. Drinking water was used for mixing and curing all test specimens. Super-plasticizer having high range water reducer was used for the fabrication of the concrete mixes. The specific gravity of the super-plasticizer was 1.15.

Steel Fiber: Hooked end and corrugated are two shapes of steel fibers that were used in this study. Figure (2) shows the photos of the steel fibers. The young's modulus, the tensile strength and the density of the steel fibers were 2100 t/cm^2, 6500 kg/cm^2 and 7.85t/m^3, respectively. The physical properties of the steel fibers are summarized in Table (3).

2.3 Concrete Mix Details

Table (4) shows the mix proportions of the three different concrete mixes. The absolute volume method was used to design the concrete mixes. Dry components of the concrete were mixed in a rotary mixer for 2 minutes. Then, steel fibers were spread slowly and continuously into the mixer to ensure a proper fiber distribution without balling. Water and super-plasticizer were added slowly and the concrete components were mixed for another 3 minutes. The steel fibers weight 4.4, 8.8 and 13.2 kg/m^3 were added to the concrete mixes with a volume percentage 0.15, 0.30 and 0.45 %, respectively. For every concrete batch, 3 cubes and 3 cylinders were prepared to determine the compression strength and the splitting tensile strength of the concrete specimens. One day after the concrete casting, all specimens were kept in water curing tanks for 28 days.

2.4 Test set up

Push-off tests on specimens were used to investigate the shear response of the steel fiber concrete.

2.4.1 Static Loading

The test setup was identical for the first 63 specimens which were tested under direct static shear load. Two linear variable displacement transformers (LVDT) were attached to the specimens to detect the vertical and the horizontal displacements along the shear plan. The positions of the LVDT^s as well as the loading configuration are shown in Fig. (3). A universal testing machine of capacity 30 tones was used for the push-off tests.

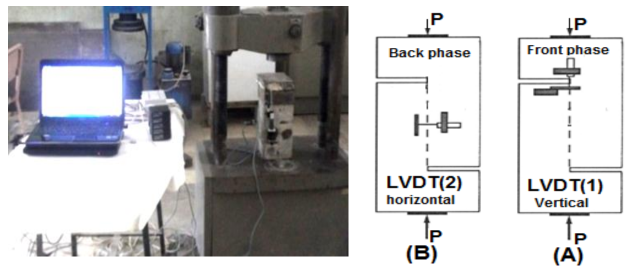

Fig. (3): Static load configuration.

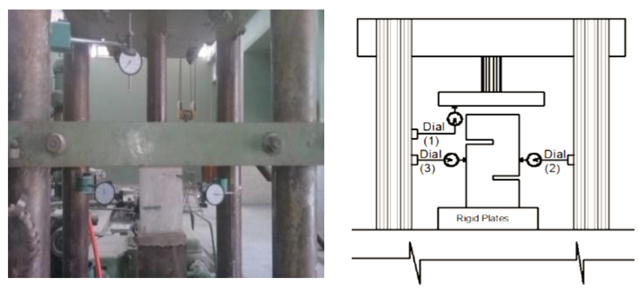

Fig. (4): Repeated test instrumentation**.**

2.4.2 Repeated loading

One type of cyclic tests was carried out with a fixed frequency rate 500 cycles per minute. The load was applied for a prefixed displacement 0.50 mm stroke to evaluate the cyclic degradation of the elements. The maximum stress level was taken to be 80 % of the ultimate static shear stress in order to ensure that all specimens fail in low cycle repeated load. The number of cycles was less than 10^4 cycles. Three dial gauges were attached to the test specimens. One vertical dial gauge was used to control the stroke limit and to inform the vertical displacement, the other two gauges were used for catching the horizontal displacement, as shown in Figure (4).

The test protocol and the properties of the repeated load are shown in Figure (5). The maximum stress ($б_{max}$) equal 80 % of the static shear stress at failure and the minimum stress ($б_{min}$) is a constant stress due to machine Jaw own weight. Table (5) shows the parametric conditions of the repeated loads.

3 Test Results and Discussion
3.1 Concrete Properties

A compression test machine (100 tones capacity) was used to conduct the compression and splitting tensile strength tests for the concrete cubes and cylinders, respectively. The results for each specimen are based on an average of three replicate elements. The presence of low dosage steel fibers enhanced the compression and splitting tensile strength for the test specimens as shown in Table (5).

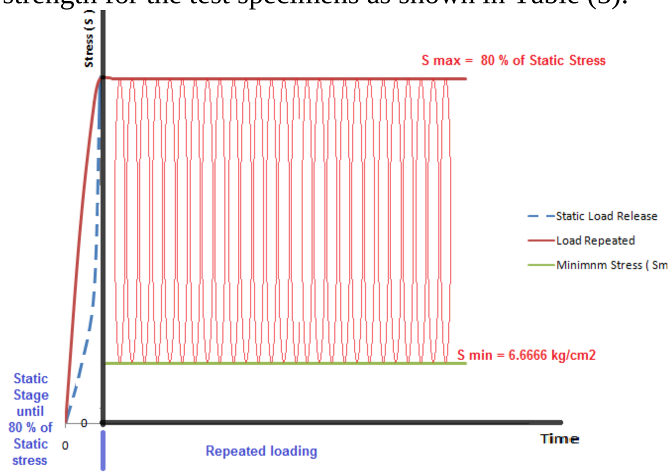

Fig. (5): Repeated test protocol.

Table (4): The stress limitations for the repeated load.

Specimens	σ min kg/cm^2	σ max kg/cm^2	σ mean* kg/cm^2
Ar1	6.67	31.10	18.90
Ar2 , Ar3	6.67	35.30	20.90
Ar4, Ar5	6.67	37.20	21.90
Ar6 , Ar7	6.67	39.10	22.90
Br1	6.67	40.20	23.40
Br2 , Br3	6.67	41.50	24.10
Br4, Br5	6.67	46.10	26.40
Br6, Br7	6.67	46.70	26.70
Cr1	6.67	48.90	27.80
Cr2 ,Cr3	6.67	51.20	28.90
Cr4, Cr5	6.67	55	30.80
Cr6, Cr7	6.67	56.90	31.70

*The mean stress = 0.50 ($б_{min}$+ $б_{max}$)

3.2 Push off Test Specimens Subjected to Static Loading

3.2.1 Patterns of cracks and modes of failure

Figures (6, 7 and 8) show the patterns of cracks for some representative specimens of each group. Test specimens were designed to fail through a defined plan (plan connecting the two parts of the Z specimen) that is subjected to a direct static shear stress. During the push off test, constant loading rate was applied to the specimens that showed no cracks. Increasing the applied loads, two cracks were concurrently initiated at the top and the bottom edges of the shear plan. Soon after their formation, the cracks were extended upward and downward resulting in the separation of the two main parts and the failure of the test specimens. For all specimens, the time period between the formation of the first visible cracks and the failure was too short (about 3 seconds) so that it was difficult to detect the exact value of the cracking load.

Generally, the increase of the concrete compressive strength and the presence of the steel fibers resulted in a delay for the formation of the first visible cracks. For specimens in category Cs (400 kg/cm^2 compressive strength), the cracks pass through the aggregate and resulted in trans-granular type of failure. However, the cracks run around the aggregates for the specimens in categories (As) and (Bs) that have compressive strength 250 and 325 kg/cm^2, respectively. It is worth to mention that, the failure of all SFC specimens resulted in a pull out for the steel fibers as shown in Figure (9).

Figure (6) Patterns of cracks for specimens in category (As)

Figure (7) Patterns of cracks for specimens in category (Bs)

Figure (8) Patterns of cracks for specimens in category (Cs)

Figure (9) Pulled out steel fiber.

3.2.2 Ultimate shear strength

The push off tests was preceded with a constant static loading rate on the specimens until failure occurred and the ultimate load was recorded. The ultimate shear strength was calculated as a result of dividing the ultimate load by the shear plan area. The concrete shear strength for all test specimens is plotted in Figures (10) and (11). Concrete specimens have 0.15, 0.30 and 0.45 volume percentages of steel fibers recorded improvements for the values of the shear strength up to 15.5%, 19.6% and 25.5%, respectively. The presence of the steel fibers was

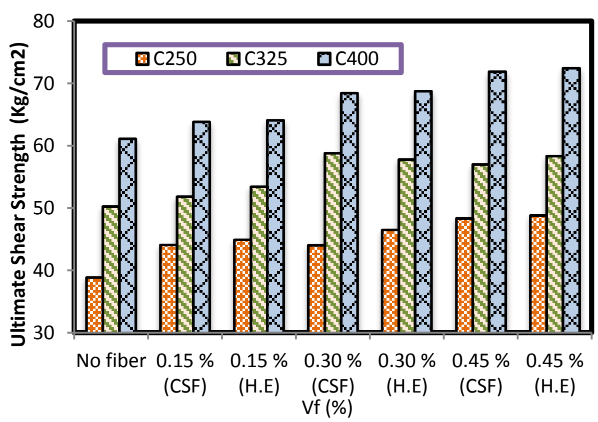

found to be more profitable for the specimens in groups A_s and B_s that have lower concrete strength.

For concrete specimens that have no steel fiber, the increase of the concrete compressive strength from 250 kg/cm^2 to 400 kg/cm^2 resulted in 57% increase for the concrete shear strength. However, the inclusion of 0.45% of steel fibers for specimen C_{s7} (C400) resulted in 86.5% increase for the concrete shear strength when compared with specimen A_{s1} (C250) that have no fibers. Compared with the specimens have corrugated steel fibers (CSF), up to 5% increase for the shear strength were recorded for the concrete specimens that have hooked end steel fiber type (H.E).

.

Figure (10): ultimate shear strength.

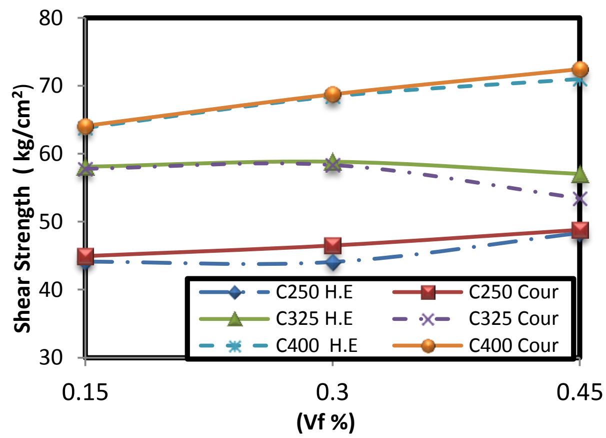

Figure (11): Effect of steel fibers on shear strength.

3.2.3 Comparison between the experimental and the predicted values of the ultimate shear strength

As the direct shear strength equation derived by the Egyptian code does not take into account the effect of the presence of the steel fiber, the experimental test results were compared with three different shear equations from previous researches, see Figures (12 to 17), and Table (5).

Khaloo and Kim (15) carried out an experimental investigation to assess the behavior of steel fiber concrete under direct shear. Equation (1) was proposed to predict the shear transfer strength of the tested specimens:

$$\mathcal{V}u = (0.65 + 0.123\,\mathcal{V}f + 0.08\,\mathcal{V}f^2 - 0.013\,\mathcal{V}f^3)\sqrt[2]{fc''} \quad (N/mm^2) \quad (1)$$

A.Khanlou (16) suggested an empirical shear transfer model to predict the ultimate shear strength of SFRC, expressed as:

$$\mathcal{V}u = 0.75\sqrt[2]{fc''} + 4\mathcal{V}f^{0.90} \quad (N/mm^2) \quad (2)$$

J.R. Al-Feel and B.J. Al Sulayvani (17) proposed equation (3) that predicts the shear strength in a determined failure plane:

$$\mathcal{V}u = 0.87\sqrt[2]{f c''} + 0.87\ \rho\mathcal{V}f + 0.90\ \sigma u + 3.33\ \mathcal{V}f * lf/df \quad (N/mm2) \quad (3)$$

The predicted values of the maximum shear strength calculated by the equations of Khaloo et al. (15) and A. Khanlou (16) were conservative when compared with the experimental values of the elements in category As (concrete compressive strength equal 250 kg/cm^2). However, these equations give highly under estimation for the values of the maximum shear strength for the elements in categories Bs and Cs that have concrete compressive strength equal 325 and 400 kg/cm^2, respectively. The percentages of the predicted to the experimental values of the ultimate shear strength were ranged from 68% to 86%. The mean and standard deviation for the predicted values of maximum shear strength using equations (1) and (2) were 2.98, 13.64 and 2.59, 11.87 respectively.

For all concrete specimens (250, 325 and 400 kg/cm^2), the predicted values of the ultimate shear strength given by J.R. Al-Feel et al. (17) were close to the experimental values as the percentages of the predicted to the experimental values were ranged from 93% to 107%, see Figures (12) to (17). The mean, standard deviation and variance were 0.41, 1.88 and 3.53, respectively.

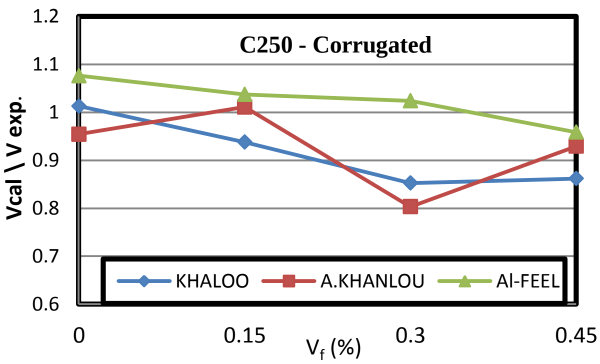

Figure (12): $V_{cal.}/V_{exp.}$ Verses the volume percentages for CSF (category (As)).

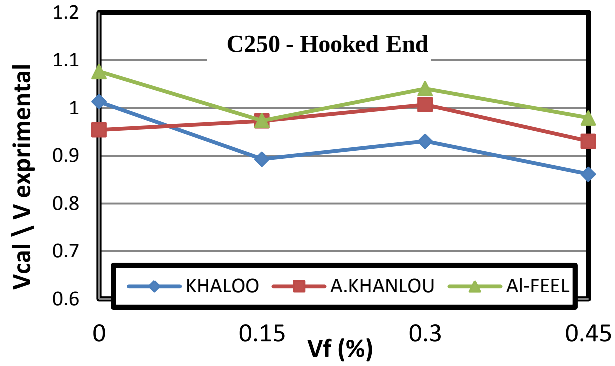

Figure (13): $V_{cal.}/V_{exp.}$ Verses the volume percentages for (category (As)).

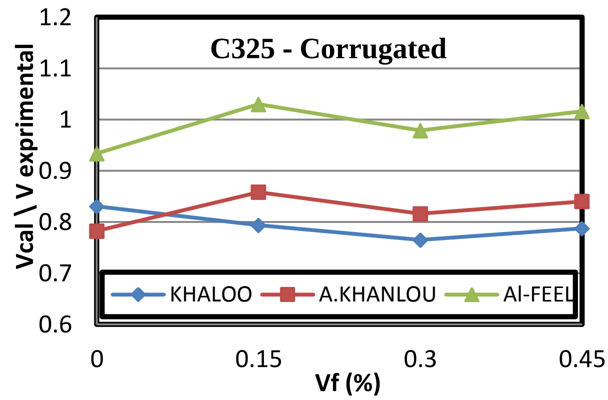

Figure (14): $V_{cal.}/V_{exp.}$ Verses the volume percentages for (category (Bs)).

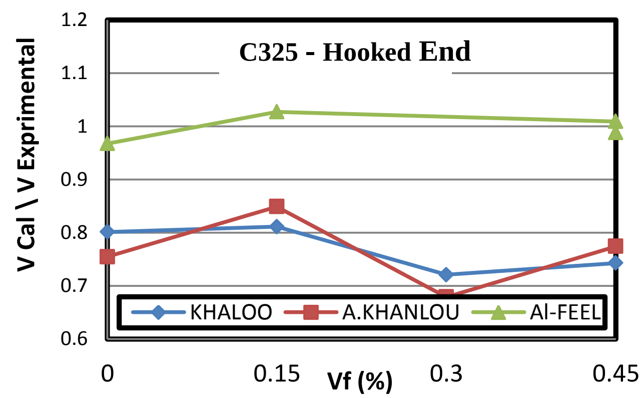

Figure (15) :$V_{cal.}/V_{exp.}$ Verses the volume percentages for (category (Bs)).

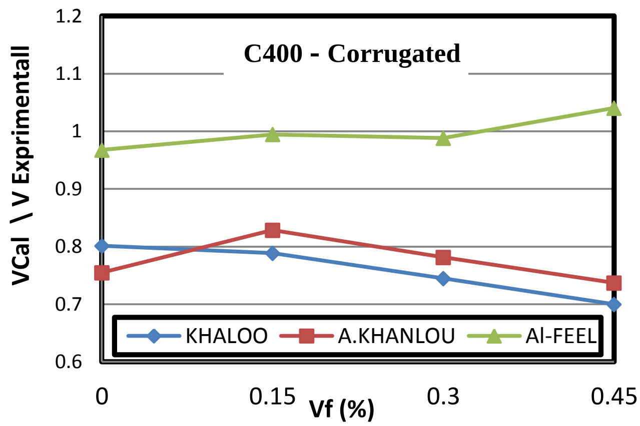

Figure (16): $V_{cal.}/V_{exp.}$ Verses the volume percentages for (category (Cs)).

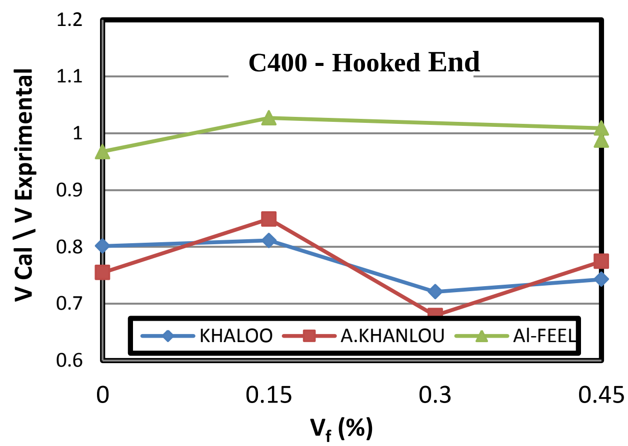

Figure (17): $V_{cal.}/V_{exp.}$ Verses the volume percentages for (category (Cs)).

Table (5): Predicted shear strength

Specimen	$V_{u\ Exp}$ (kg/cm^2)	$V_{cal.}$ / $V_{Exp.}$ Khaloo et al.(15)	A.Khanlou (16)	Al-Feel (17)
As1	38.86	1.01	0.95	1.07
As2	44.13	0.89	0.97	0.97
As3	44.94	0.94	1.01	1.03
As4	44.08	0.93	1.01	1.04
As5	46.50	0.85	0.80	1.02
As6	48.34	0.86	0.93	0.98
As7	48.80	0.86	0.93	0.96
Bs1	50.28	0.83	0.78	0.93
Bs2	51.86	0.79	0.86	1.02
Bs3	53.46	0.79	0.86	1.01
Bs4	58.84	0.76	0.82	0.98
Bs5	57.80	0.72	0.68	0.99
Bs6	57.04	0.78	0.84	1.02
Bs7	58.35	0.73	0.79	0.93
Cs1	61.11	0.80	0.75	0.97
Cs2	63.82	0.79	0.83	0.99
Cs3	64.11	0.81	0.85	1.03
Cs4	68.44	0.74	0.78	0.99
Cs5	68.75	0.72	0.68	1.01
Cs6	71.88	0.70	0.74	1.04
Cs7	72.47	0.74	0.77	0.99

3.2.4 Displacement

The horizontal and vertical displacements were measured by a linear variable displacement transformer (LVDT) along the shear plan.

3.2.4.1 Vertical displacement

The values of the maximum vertical displacement for the tested specimens were measured and plotted in Figures (18) and (19) for the specimens have corrugated and hooked end steel fibers, respectively. It is clear that, the increase of the volume percentage of both types of the steel fibers increases the maximum values of the vertical displacements (up to 49%) indicting improvements for the specimens' ductility. It could be observed that the corrugated fibers showed slightly higher values of maximum vertical displacement than the hooked end steel fibers. For all tested specimens, the values of the maximum vertical displacements were found to be inversely affected by the increase of the concrete compressive strength. Increasing the concrete compressive strength from 250 kg/cm^2 to 400 kg/cm^2 resulted in up to 19.6% decrease for the values of the maximum vertical displacements.

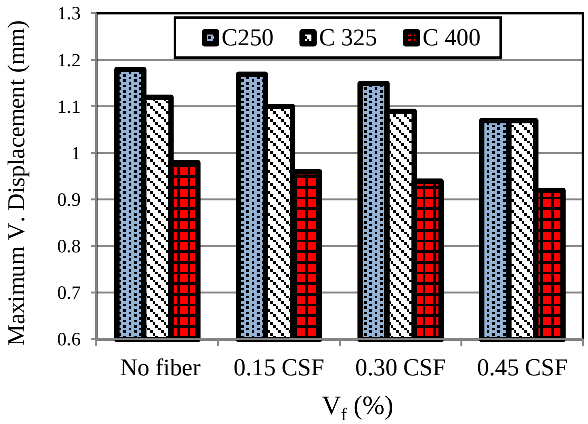

Figure (18): Max. Vertical displacement for (CSF).

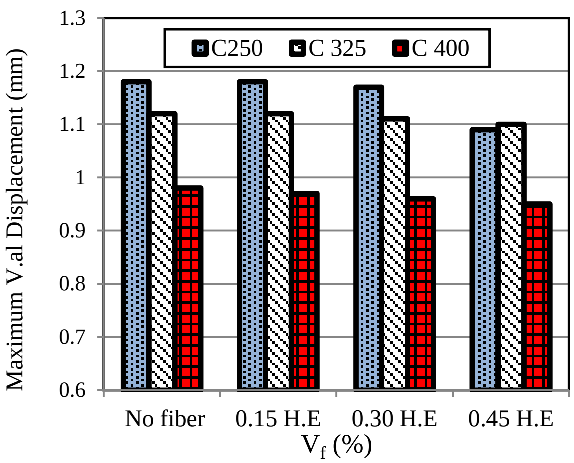

Figure (19): Max. vertical displacement (HESF).

3.2.4.2 Horizontal displacement

Figures (20) and (21) show the maximum horizontal displacements that are found to be (25% to 45%) higher than the maximum vertical displacements. Similar to the vertical displacements, the horizontal displacements were positively affected by the presence of the steel fiber. Increasing the volume percentages of the steel fibers from 0% to 0.45% (by volume) resulted in up to 37% increase for the horizontal displacement. The steel fibers allowed the tested specimens to withstand higher values of deformation and ductility before the final failure. It is worth to mention that the presence of corrugated instead of hooked end steel fiber resulted in slightly higher values of horizontal displacements. The increase of the concrete compressive strength from 250 to 400 kg/cm^2 resulted in up to 22% decrease for the values of the maximum horizontal displacements.

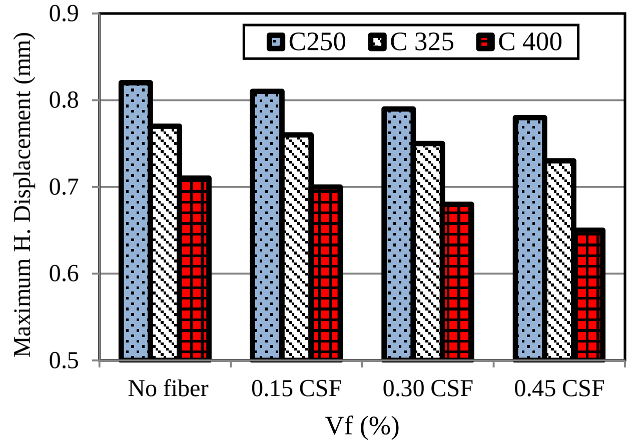

Figure (20): Max. horizontal displacement for (CSF).

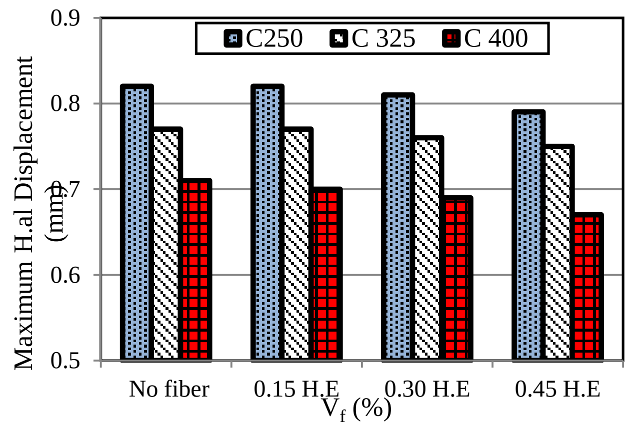

Figure (21): Max. horizontal displacement for (HESF).

3.3 Push off Test Specimens Subjected to Repeated Loading

3.3.1 Patterns of Cracks and Modes of Failure

Figures (22, 23 and 24) show the patterns of cracks and modes of failure for some representative specimens of groups A_r, B_r and C_r, respectively. During the push off test, the repeated load was applied with a constant amplitude rate (500 cpm). Modes of failure and cracking scenarios were the same for all specimens. The first crack initiated on the top and the bottom edges of the shear plan (beside grooves). The cracks were propagated upward and downward the shear plan resulting in the direct shear failure of the tested specimens. The time elapsed between the formation of the first crack and the failure of the specimens was too short. The failure surface was inspected, fibers were picked off from one side of the concrete; but, no deformations in steel fiber were recorded. For category (C_r) (concrete compressive strength equal 400 kg/cm^2), a trans-granular fracture was occurred, the cracks pass through grains. However, an inter-granular fracture happened for the specimens of categories (A_r) and (B_r). The crack propagation was around the grain boundaries through the weaken mortar.

Figure (22): Pattern of cracks for category (Ar).

Figure (23): Pattern of cracks for category (Br).

Figure (24): Pattern of cracks for category (Cr).

3.3.2 Fatigue Life and S-N Diagrams:

Table (6) and Figures (25 to 28) show the fatigue life for all tested specimens. It is clear that, the increase of the concrete compressive strength highly increases the fatigue life for all tested specimens. The increase of the concrete compressive strength from 250 kg/cm^2 to 325 kg/cm^2 resulted in up to 97% increase for the fatigue life. On using concrete compressive strength 400 kg/cm^2 for casting the tested specimens, the percentages of increase of the fatigue life were up to 224%.

Using low dosages of steel fibers 0.15%, 0.3% and 0.45% by volume resulted in up to 20.8%, 51% and 82% increase of the fatigue life for the tested specimens. The highest percentages of increase of the fatigue life due to the presence of the steel fibers were recorded for the specimens casted with 250 kg/cm^2 concrete compressive strength. Compared with the corrugated steel fibers, test results showed that the use of hooked end steel fibers resulted in an increase from 3.3% to 16.86% of the fatigue for the tested specimens.

The presence of the steel fibers enabled the push-off test specimens to increase its fatigue life by increasing shear plan rigidity. The fiber bridging and fiber pullout dissipates energy required for the initiation of the crack within the shear plan. The cyclic stress cumulating plays a dominant role in crack growth and therefore takeover the fatigue life for SFC specimens. Steel fibers support the shear plan to resist the early deterioration of section by keeping the gross inertia that affects the fatigue life.

Table (6): Fatigue life for test specimens.

Category	Specimens	No. of cycles
A_r	A_{r1}	788
	A_{r2}	952
	A_{r3}	891
	A_{r4}	1187
	A_{r5}	1076
	A_{r6}	1434
	A_{r7}	1381
B_r	B_{r1}	1554
	B_{r2}	1809
	B_{r3}	1622
	B_{r4}	2094
	B_{r5}	1845
	B_{r6}	2481
	B_{r7}	2122
C_r	C_{r1}	2547
	C_{r2}	2935
	C_{r3}	2752
	C_{r4}	3855
	C_{r5}	3454
	C_{r6}	4308
	C_{r7}	4169

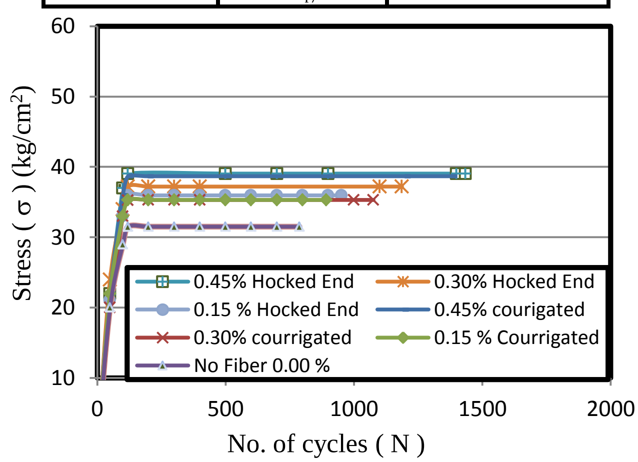

Figure (25): (S – N) diagrams for category (Ar).

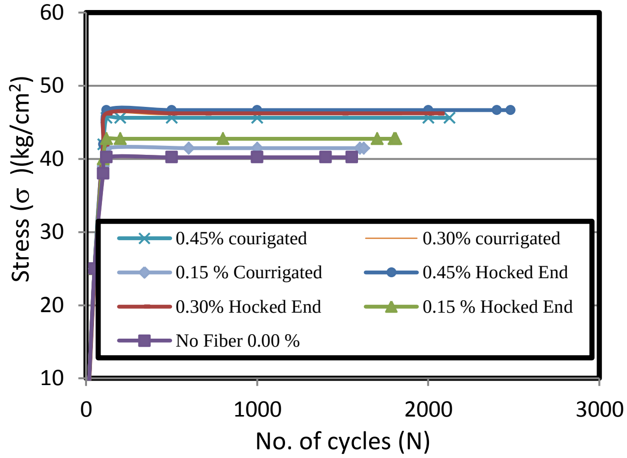

Figure (26): (S – N) diagrams for category (Br).

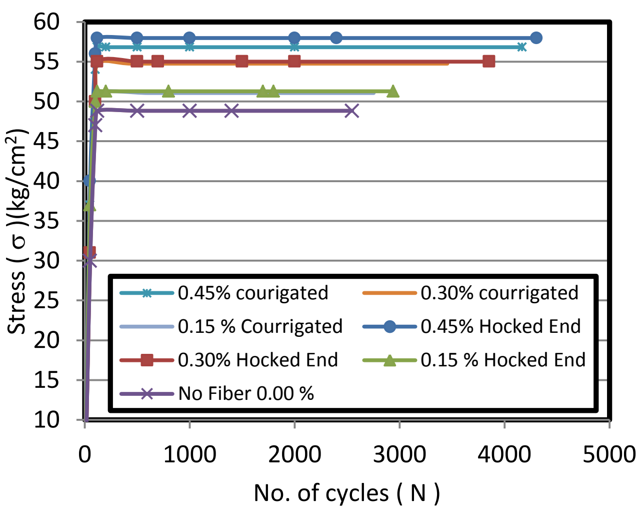

Figure (27): (S – N) diagrams for category (Cr).

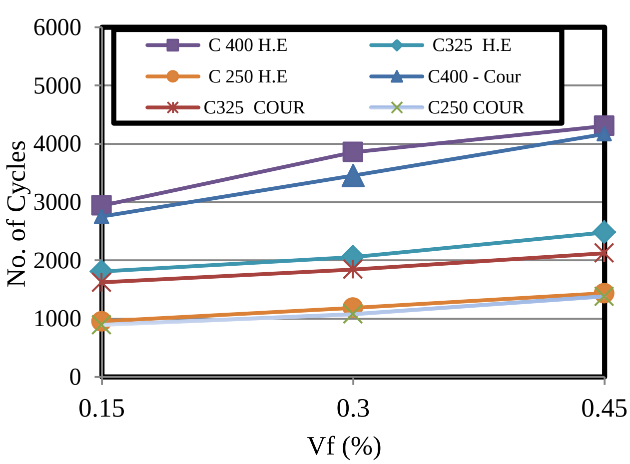

Figure (28): No. of cycles vs. fiber content.

3.3.3 Displacement

3.3.3.1 Horizontal Displacements

Figures (29), (30) and (31) show the relationship between the number of load cycles and the horizontal displacement for the test specimens in groups (A_r), (B_r) and (C_r), respectively. Generally, it is clear that, for the same number of load cycles, the horizontal displacement decreases with the increase of the volume percentage of the steel fibers. At a certain number of cycles, the presence of a low dosage of corrugated steel fibers and hooked end steel fibers resulted in up to 19.34% and 16.19% decrease for the values of the maximum horizontal displacement respectively. However, the increase for the volume percentages of the steel fibers resulted in higher values of maximum horizontal displacement at failure. It is worth to mention that the increase of the concrete compressive strength reduced the values of the horizontal displacements.

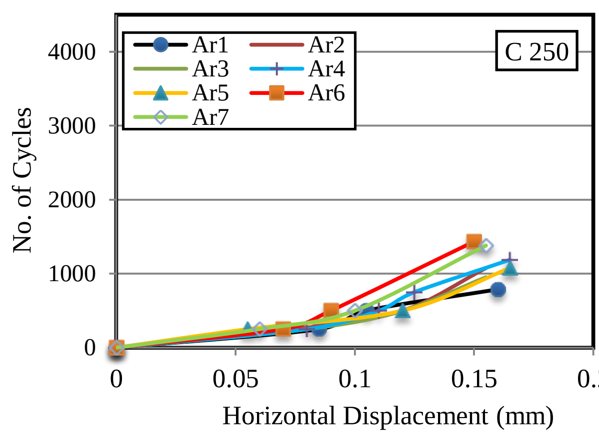

Figure (29): Horizontal displacement for category (Ar).

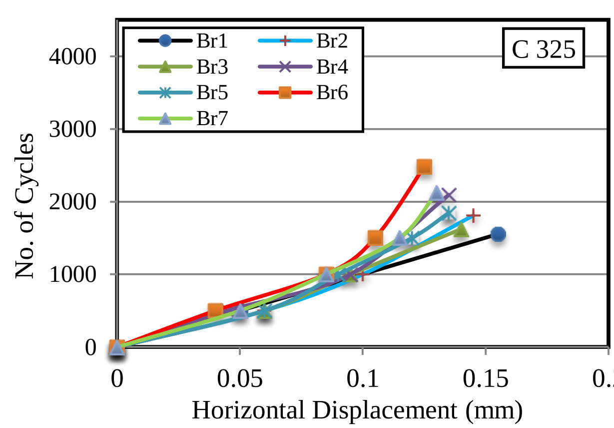

Figure (30): Horizontal displacement for category (Br).

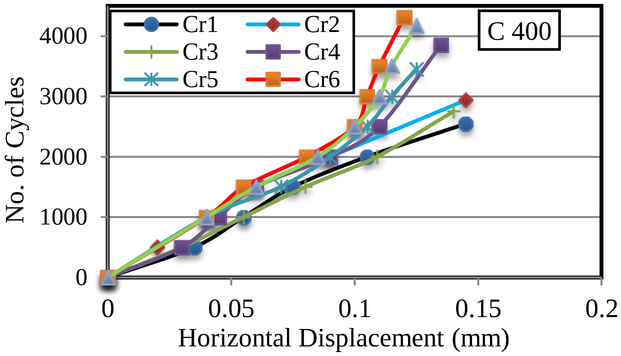

Figure (31): Horizontal displacement for category (Cr).

3.3.3.2 Vertical Displacement

Figures (32), (33) and (34) shows the relationship between the number of load cycles and the vertical displacement. At a certain number of cycles, the vertical displacement was found to be decreased with the increase of the volume percentages of the steel fibers. Increasing the fiber content from 0 to 0.45 % resulted in up to 12.19 % decrease for the maximum vertical displacement which is attributed to the ability of the steel fiber to control the crack width.

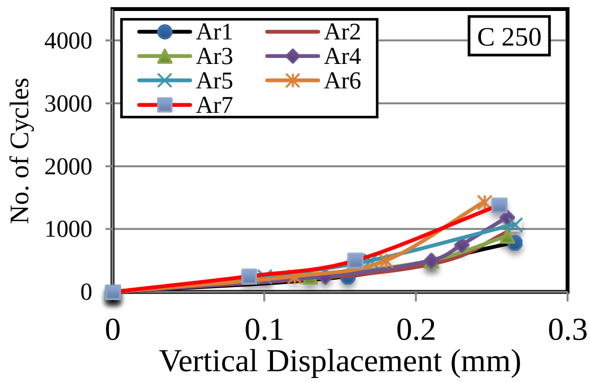

Figure (32): Vertical displacements for category (Ar).

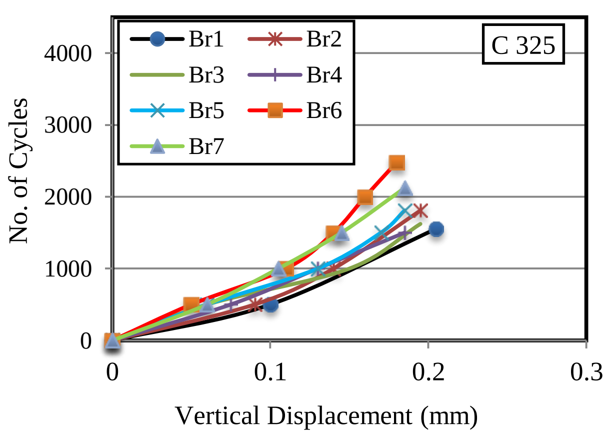

Figure (33): Vertical displacements for category (Br).

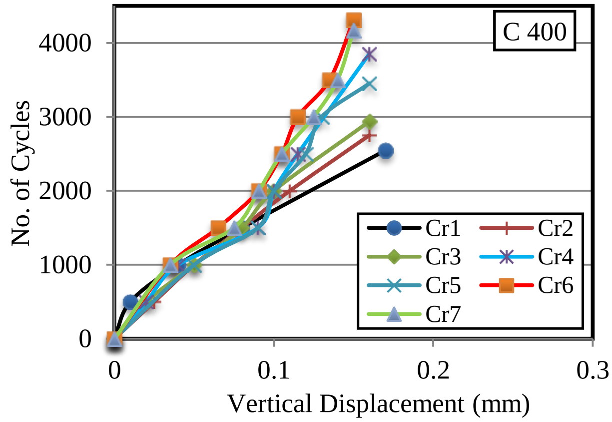

Figure (34): Vertical displacements for category (Cr).

3.3.4 Suggested Equation to predict fatigue life

Using a regression analysis for the fatigue test results of the concrete specimens, the authors propose the following equation to predict the No. of cycles for the concrete specimens have low dose steel fiber content and subjected to direct shear stresses.

$$\boldsymbol{No.\ of\ cycles} = \mathbf{0.70}\sqrt{\boldsymbol{fcu}} + \mathbf{0.53}\,\boldsymbol{Vf}(\boldsymbol{Lf}\backslash\boldsymbol{Df}) + \mathbf{0.8}\,\boldsymbol{Smax}(\mathbf{0.85} + \mathbf{0.446}\,\boldsymbol{Smax} + \mathbf{0.014}\,\boldsymbol{Smax}^{\mathbf{2}})$$

The equation takes into account the concrete compressive strength (f_{cu}), maximum stress level (S_{max}), the volume percentage of fibers (V_f) and the aspect ratio of the steel fibers ($L_f \backslash D_f$). The predicted values of the No. of cycles showed good agreement with the experimental test results as shown in Figures from (35) to (37). The percentages of the difference between the predicted and the experimental values of the number of load cycles were ranged from -13% to +4%.

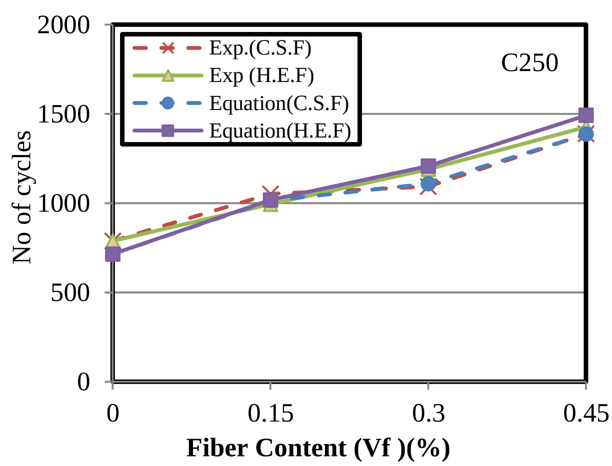

Figure (35): Predicted and experimental values of the No. of cycles for test specimens in category A_r.

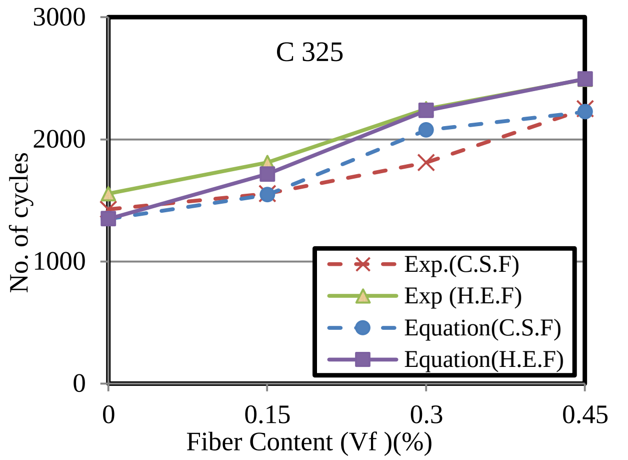

Figure (36): Predicted and experimental values of the No. of cycles for test specimens in category B_r.

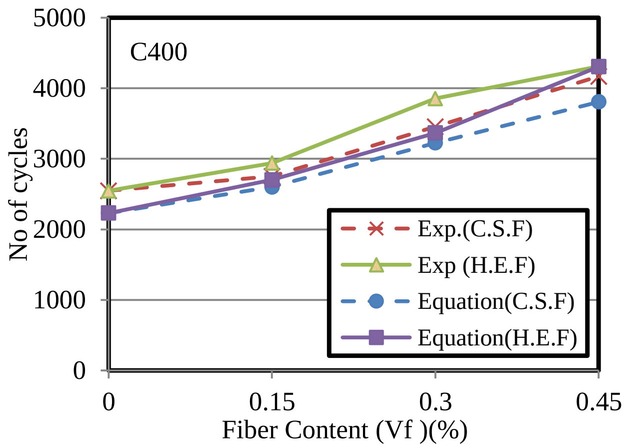

Figure (37): Predicted and experimental values of the No. of cycles for test specimens in category C_r.

4. Conclusions

1- All concrete push off tested specimens were failed due to shear stresses through a defined shear plan. The concrete specimens subjected to static loads that have 0.15, 0.30 and 0.45 volume percentages of steel fibers showed 15.5%, 19.6% and 25.5% increase for the values of the shear strength respectively.

2- Compared with the concrete specimens subjected to static loads and have corrugated steel fibers (CSF), up to 5% increase for the shear strength were recorded for the concrete specimens that have hooked end steel fiber.

3- Compared with the experimental values of the test specimens in category As, the predicted values of the maximum shear strength calculated by equations of Khaloo et al. (15) and A.Khanlou (16) were conservative. However, these equations give under estimation for the values of the maximum shear strength for the elements in categories Bs and Cs that have concrete compressive strength equal 325 and 400 kg/cm^2, respectively. The percentages of the predicted to the experimental values of the ultimate shear strength were ranged from 68% to 86% . The standard deviation of the predicted values of khaoo et al. and A Khanlou were 13.64 and 11.87, respectively.

4- For all test specimens, the predicted values of the ultimate shear strength given by J.R. Al-Feel et al. (17) equation showed good agreement with the experimental values as the difference between the predicted to the experimental values were in the range of ±7%. The mean and standard deviation were 0.41 and 1.88, respectively.

5- The presence of the steel fibers enables to increase the fatigue life of the push-off test specimens. Using low dosages of steel fibers 0.15%, 0.3% and 0.45% by volume resulted in 20.8%, 51.0% and 82.0% increase for the fatigue life of the test specimens. The highest percentages of increase for the fatigue life were recorded for the specimens casted with 250 kg/cm^2 concrete compressive strength.

6- Test results showed that the use of the hooked end instead of the corrugated steel fibers resulted in an increase from 3.3% to 16.86% for the fatigue life of the test specimens.

7-The authors propose an empirical equation that showed good agreement for the prediction of the number of load cycles for the concrete specimens that have low volume percentages of steel fiber and subjected to direct shear stresses.

5. REFERENCES

1- Higashiyama, H., & Banthia, N. 2008. "Correlating flexural and shear toughness of lightweight fiber-reinforced concrete" ACI Materials Journal, Vol. 105(3), pp. 251-257.
2- Majdzadeh, F., Soleimani, S. M., & Banthia, N. 2006 "Shear strength of reinforced concrete beams with a fiber concrete matrix" Canadian Journal of Civil Engineering, Vol. 33(6), pp. 726-734.
3- Mirsayah, A. A., & Banthia, N. 2002 "Shear strength of steel fiber-reinforced concrete" ACI Material Journal vol. 99 (5), pp. 473-479.
4- Valle, M., & Buyukozturk, O. 1993. "Behavior of fiber reinforced high-strength concrete under direct shear" ACI Materials Journal, Vol. 90(2), pp. 122-133.
5- Narayanan, R., & Darwish, I. Y. S. 1987 "Use of steel fibers as shear reinforcement" ACI Structural Journal, Vol. 84 (3), pp. 216-227.
6- RILEM Technical Committee TC 36-RDL. Long term random dynamic loading of concrete structures. Mater. Struc. 1984;17(97), pp.1‑28.

7- Miguel Fernandez Ruiz, Carlos Zanuy, Francisco natareo, Juan Manuel Gallego, Luis Albajar and Aurelio Muttoni (2015) "Influence of fatigue loading in shear failures of reinforced concrete members without transverse reinforcement" Journal of Advanced Concrete Technology. Vol.13, pp. 263–274.

8- Esayas Gebreyouhannes, Toshiharu Kishi and Koichi Maekawa review (2008) "Shear fatigue response of cracked concrete interface" Journal of Advanced Concrete Technology, Vol.6, No.(2), pp. 365–376.

9- Jun Wei Luo and Frank Vecchio review (2016) "Behavior of Steel Fiber-Reinforced Concrete Under Reversed Cyclic Shear" ACI Structural Journal, Vol. 113, No. (1), pp.75-84.

10- Harish Kumar N. R., Jagannath L, K.P Nagaraj and R. Prabhakara (2015) "Evaluation of In-plane Shear Strength in SCC Using Inclined Plane Push–off Specimen" International Research Journal of Engineering and Technology, Vol.2, Issue :04 e-ISSN: 2395 -0056, pp. 1476-1481.

11- Mattock, A. H., & Hawkins, N. M. 1972. Shear transfer in reinforced concrete. PCI Journal, Vol. 2. (March/April) 55-75.

12- Hofbeck, J., Ibrahim, I. and Mattock, A. H. 1969. "Shear transfer in reinforced concrete" ACI Journal Proceedings, Vol. 66 – issue 2, pp. 119-128.

13- Walraven, J. C., & Reinhardt, H. W. 1981. Theory and experiments on the mechanical behavior of cracks in plain and reinforced concrete subjected to shear loading. HERON, Vol. 26(1).

14- Javier Echegaray-Oviedo, Juan Navarro-Gregori, Estefania Cuenca and Pedro Serna, (2013) "Upgrading the push-off test to study the mechanisms of shear transfer in FRC elements" VIII International Conference on Fracture Mechanics of Concrete and Concrete Structures, Spain, pp. 1-10.

15- Khaloo,A.R. and KIM,N.(1997). Influence of concrete and fiber characteristics on behavior of steel fiber concrete. ACI Materials Journal, 94 (6) , 596-601.

16- A.Khanlou, G. A. MacRae , A. N. Scott , S. J. Hicks and G. C. Clifton (2013) "Shear performance of steel fiber reinforced concrete" Steel Innovation Conference, New Zealand.

17- J. R. Al-Feel and B.J.AL-Sulayvani (2009) "Effect of direct compressive stress on the shear transfer strength of fibrous concrete" Al Rafidain Engineering Journal, Vol.17, No.2, pp. 66-76.

18- ECP 203-2017, Egyptian Code of Practice for Design and Construction of Reinforced Concrete Structures ECP-203, Housing and Building Research Center, Ministry of Building and Construction, Giza, Egypt, 2017.

19- Valle, M., & Buyukozturk, O. 1993. Behavior of fiber reinforced high-strength concrete under direct shear. ACI Materials Journal, Vol. 90(2) 122-133.